INTERNATIONAL JOURNAL FOR NUMERICAL METHODS IN FLUIDS, VOL. 9, 289–303 (1989)

FINITE ELEMENT SOLUTION OF AN ENCLOSED TURBULENT DIFFUSION FLAME

A. C. BENIM

Institut für Verfahrenstechnik und Dampfkesselwesen, University of Stuttgart, D-7000 Stuttgart 80, Federal Republic of Germany

SUMMARY

A finite element formulation of enclosed turbulent diffusion flames is presented. A primitive variables approach is preferred in the analysis. A mixed interpolation is employed for the velocity and pressure. In the solution of the Navier–Stokes equations, a segregated formulation is adopted, where the pressure discretization equation is obtained directly from the discretized continuity equation, considering the velocity–pressure relationships in the discretized momentum equations. The state of turbulence is defined by a k–ε model. Near solid boundaries, a wall function approach is employed. The combustion rates are estimated using the eddy dissipation concept. The expensive direct treatment of the integrodifferential equations of radiation is avoided by employing the moment method, which allows the derivation of an approximate local field equation for the radiation intensity. The proposed finite element model is verified by investigating a technical turbulent diffusion flame of semi-industrial size, and comparing the results with experiments and finite difference predictions.

KEY WORDS Enclosed turbulent diffusion flames Finite elements Segregated formulation k–ε turbulence model Eddy dissipation concept Moment method

INTRODUCTION

Today's topical problems in combustion engineering, such as the reduction of pollutant formation while retaining the combustion efficiency, have brought about a renewed interest in the development of detailed prediction procedures for flames. This is of course also supported by the recent improvements in computational facilities, which render the use of increasingly realistic mathematical models and more powerful numerical techniques possible. The prediction procedures which are currently being employed for technical flames are almost exclusively based on finite difference methods.[1] The basic advantage of the finite element method is to allow for a flexible mesh. Thus the discretization can be adjusted to the geometry and the characteristics of the problem in a natural way. Mapping methods, which are being explored for finite difference codes,[2] do not provide the same degree of flexibility. The solutions of turbulent reacting flows exhibit very sharp gradients of the field variables. Further, the real burner shapes involve fine geometrical details which influence the near-field flow decisively. Therefore this flexibility of the finite element method can be expected to prove useful in flame prediction procedures. For this reason, we believe that it is worthwhile to study the application of the finite element method to technical flames. This is the scope of the present investigation.

0271–2091/89/030289–15$07.50

Received 18 January 1988
Revised 13 May 1988

Some applications of the finite element method in combustion problems have recently been reported. Sohn and Chung[3] have investigated the development of unstable waves in rocket motor chambers. Benkhaldoun and Larrouturou[4] have computed the flame propagation in a reactive–diffusive system, neglecting the coupling to the flow field, using an adaptive grid. Murray and Carey[5] have studied the transport of chemical components within a laminar flow field with chemical reactions taking place at the solid boundary. Habbal *et al.*[6] have presented a finite volume/finite element mixed procedure for the computation of flame propagation within an ignitable gaseous mixture where the flow field is assumed to be inviscid.

In this paper we present a finite element formulation of enclosed turbulent diffusion flames. Turbulent diffusion flames are encountered in many important engineering applications, such as furnaces of thermal power plants, industrial furnaces or gas turbine combustors. The fuel and oxidant are injected separately into the combustion chamber, where they are mixed with each other and with the recirculating hot combustion products within a turbulent flow field and react with intensive heat release.

The turbulence here is primarily responsible for the all important mixing and convective transport processes. Therefore it is a very important feature of the flow. Previous experience indicates that the inexpensive algebraic turbulence models are not accurate enough for this class of problems. In the present analysis the turbulence state is defined by a k–ε model,[7] which provides an optimal choice between accuracy and economy for practical purposes. Near solid boundaries, due to modelling difficulties caused by relaminarization effects, a wall function approach[7] is used, where the flow in the near-wall region is not solved for but is assumed to obey the so-called 'law of the wall'. Finite element applications of the k–ε model and the method of wall functions in isothermal flow problems were presented in a previous paper.[8]

In technical flames, besides convection, another mode of heat transfer, namely radiation, also becomes important. The radiative transfer is governed by integrodifferential equations. Thus the efficient 'sparse matrix' type of numerical procedure for convective transport cannot readily be employed to handle the radiation. Direct discretization procedures[9] to treat the equations of radiation require too much computer time and storage[10] to allow them to be coupled with the iterative convective flow solution. In finite difference codes the so-called 'flux methods'[10] are exclusively employed as radiation models, which are differential approximations derived under certain assumptions concerning the directional variation of the radiation intensity. Nevertheless, conventional flux methods are principally not compatible with irregular geometries and meshes. Therefore they do not provide a convenient alternative for finite element formulations. For this reason another differential approximation, namely the 'moment method',[11] is employed as the radiation model in this work, since it imposes no restrictions concerning the regularity of the mesh. It was shown in a recent paper[12] that the prediction capability of the method is comparable to that of many conventional flux methods.

GOVERNING EQUATIONS

The 'mean' equations of the turbulent flow are derived by using the Reynolds-averaging approach.[13] The terms involving density fluctuations are neglected. This approximation is also in agreement with the recent experimental findings[14] demonstrating a relatively small influence of density correlation terms in turbulent diffusion flames. In the present analysis attention is focused on statistically steady and axisymmetrical systems. In the following the overbars, which are usually used to denote the Reynolds-averaged quantities, will be omitted for the sake of simplicity.

Momentum equations and the equation of continuity

Using a turbulent viscosity approach,[13] the Reynolds-averaged momentum equations can be expressed as

$$\rho\left(u\frac{\partial u}{\partial x}+v\frac{\partial u}{\partial r}\right)=-\frac{\partial p}{\partial x}+\frac{\partial}{\partial x}\left\{2\mu_e\frac{\partial u}{\partial x}-\frac{2}{3}\left[\rho k+\mu_e\left(\frac{\partial u}{\partial x}+\frac{v}{r}+\frac{\partial v}{\partial r}\right)\right]\right\}$$
$$+\frac{1}{r}\frac{\partial}{\partial r}\left[r\mu_e\left(\frac{\partial u}{\partial r}+\frac{\partial v}{\partial x}\right)\right], \tag{1}$$

$$\rho\left(u\frac{\partial v}{\partial x}+v\frac{\partial v}{\partial r}\right)=-\frac{\partial p}{\partial r}+\frac{\partial}{\partial x}\left[\mu_e\left(\frac{\partial u}{\partial r}+\frac{\partial v}{\partial x}\right)\right]+\frac{1}{r}\frac{\partial}{\partial r}\left\{r2\mu_e\frac{\partial v}{\partial r}-r\frac{2}{3}\left[\rho k+\mu_e\left(\frac{\partial u}{\partial x}+\frac{v}{r}+\frac{\partial v}{\partial r}\right)\right]\right\}$$
$$-2\mu_e\frac{v}{r^2}+\frac{12}{r3}\left[\rho k+\mu_e\left(\frac{\partial u}{\partial x}+\frac{v}{r}+\frac{\partial v}{\partial r}\right)\right]. \tag{2}$$

The effective viscosity μ_e in equations (1) and (2) is given by

$$\mu_e=\mu+\mu_t. \tag{3}$$

The turbulent viscosity μ_t in (3) must be determined by a suitable turbulence model. The equation of continuity is

$$\rho\left(\frac{\partial u}{\partial x}+\frac{v}{r}+\frac{\partial v}{\partial r}\right)+u\frac{\partial \rho}{\partial x}+v\frac{\partial \rho}{\partial r}=0. \tag{4}$$

The turbulence model

A k–ε model of turbulence[7] is employed, in which the turbulent viscosity is related to the turbulence kinetic energy and its dissipation rate as

$$\mu_t=C_D\rho k^2/\varepsilon. \tag{5}$$

For high turbulent Reynolds numbers the transport equations for k and ε can be expressed as

$$\rho\left(u\frac{\partial k}{\partial x}+v\frac{\partial k}{\partial r}\right)-\frac{\partial}{\partial x}\left(\frac{\mu_e}{\sigma_{k,e}}\frac{\partial k}{\partial x}\right)-\frac{1}{r}\frac{\partial}{\partial r}\left(\frac{\mu_e}{\sigma_{k,e}}r\frac{\partial k}{\partial r}\right)=G_k-\rho\varepsilon, \tag{6}$$

$$\rho\left(u\frac{\partial \varepsilon}{\partial x}+v\frac{\partial \varepsilon}{\partial r}\right)-\frac{\partial}{\partial x}\left(\frac{\mu_e}{\sigma_{\varepsilon,e}}\frac{\partial \varepsilon}{\partial x}\right)-\frac{1}{r}\frac{\partial}{\partial r}\left(\frac{\mu_e}{\sigma_{\varepsilon,e}}r\frac{\partial \varepsilon}{\partial r}\right)=C_1\varepsilon G_k/k-C_2\rho\varepsilon^2/k, \tag{7}$$

where

$$G_k=\mu_t\left\{2\left[\left(\frac{\partial u}{\partial x}\right)^2+\left(\frac{\partial v}{\partial r}\right)^2+\left(\frac{v}{r}\right)^2\right]+\left(\frac{\partial u}{\partial r}+\frac{\partial v}{\partial x}\right)^2\right\}-\frac{2}{3}\left[\rho k+\mu_t\left(\frac{\partial u}{\partial x}+\frac{v}{r}+\frac{\partial v}{\partial r}\right)\right]\left(\frac{\partial u}{\partial x}+\frac{v}{r}+\frac{\partial v}{\partial r}\right). \tag{8}$$

Conservation equations for chemical components

The conservation equation of a chemical component in the gaseous mixture is given by[15]

$$\rho\left(u\frac{\partial m_j}{\partial x}+v\frac{\partial m_j}{\partial r}\right)-\frac{\partial}{\partial x}\left(\frac{\mu_e}{\sigma_{m_j,e}}\frac{\partial m_j}{\partial x}\right)-\frac{1}{r}\frac{\partial}{\partial r}\left(\frac{\mu_e}{\sigma_{m_j,e}}r\frac{\partial m_j}{\partial r}\right)=\rho S_j, \tag{9}$$

where S_j contains the source of species j due to chemical reactions and phase change. If the fuel and oxidant are injected separately as primary and secondary flows into the combustion chamber, and if it is assumed that the effective Schmidt numbers of the components are equal, the following special form of the conservation equation (9) can be obtained:[15]

$$\rho\left(u\frac{\partial f}{\partial x}+v\frac{\partial f}{\partial r}\right)-\frac{\partial}{\partial x}\left(\frac{\mu_e}{\sigma_{f,e}}\frac{\partial f}{\partial x}\right)-\frac{1}{r}\frac{\partial}{\partial r}\left(\frac{\mu_e}{\sigma_{f,e}}r\frac{\partial f}{\partial r}\right)=0. \tag{10}$$

The 'mixture fraction' f is defined as

$$f=\frac{\Phi_j-(\Phi_j)_s}{(\Phi_j)_p-(\Phi_j)_s}, \tag{11}$$

where

$$\Phi_j=\frac{m_F}{\nu_F}-\frac{m_j}{\nu_j} \tag{12}$$

for reacting components taking part in a single step combustion reaction.

The reaction model

A one-step irreversible reaction for the combustion of a gaseous hydrocarbon fuel is considered, which can be expressed as

$$|\nu_F|F+|\nu_{O_2}|O_2\rightarrow|\nu_{CO_2}|CO_2+|\nu_{H_2O}|H_2O. \tag{13}$$

The combustion rate is estimated employing the eddy dissipation concept.[16] The model assumes that the combustion rate is determined by the dissipation rate of turbulence eddies, which contain fuel, oxygen and hot combustion products and show an intermittent coexistence. Here the source term S_j in (9) for the fuel is given by

$$S_F=\nu_F\frac{\varepsilon}{k}\min\left(-C_{1,EDC}\frac{m_F}{\nu_F},-C_{1,EDC}\frac{m_{O_2}}{\nu_{O_2}},C_{2,EDC}(m_{CO_2}+m_{H_2O})\right). \tag{14}$$

The energy equation

The transport equation for the specific enthalpy can be given as[15]

$$\rho\left(u\frac{\partial h}{\partial x}+v\frac{\partial h}{\partial r}\right)-\frac{\partial}{\partial x}\left(\frac{\mu_e}{\sigma_{h,e}}\frac{\partial h}{\partial x}\right)-\frac{1}{r}\frac{\partial}{\partial r}\left(\frac{\mu_e}{\sigma_{h,e}}r\frac{\partial h}{\partial r}\right)=S_h, \tag{15}$$

where S_h takes the heat source due to radiation into account. Here the kinetic energy, pressure work and viscous dissipation terms are neglected. Assuming an 'ideal' mixture, the local mean temperature and density can be obtained from

$$T=\left(h-\sum_j\Delta h_j m_j\right)\Big/\sum_j c_{p,j}m_j, \tag{16}$$

$$\rho=p/RT\sum_j m_j/M_j. \tag{17}$$

The radiation model

Finite difference codes exclusively employ flux methods[10] as radiation models. In flux models a discrete angular distribution of the radiation intensity is assumed. This produces ordinary

differential equations for the radiative energy transport, which are to be solved along the orthogonal co-ordinate directions (along $x=\text{const.}$, $r=\text{const.}$ grid lines). Therefore the application of flux models using irregular grids seems not to be straightforward. We propose here the employment of the moment method[11] as radiation model in finite element codes, which can be used directly in irregular grids. The derivational details and some finite element applications of the method can be found in Benim.[12] Here the following approximate field equation for the radiation intensity is obtained:

$$\frac{\partial}{\partial x}\left(\frac{1}{\beta}\frac{\partial I_0}{\partial x}\right)+\frac{1}{r}\frac{\partial}{\partial r}\left(\frac{1}{\beta}r\frac{\partial I_0}{\partial r}\right)=3K_a[I_0-I_b(T)]. \tag{18}$$

Assuming grey walls, the following boundary condition for (18) can be derived:

$$\frac{\partial I_0}{\partial n}+\frac{3\beta\varepsilon_w}{2(2-\varepsilon_w)}(I_0-I_{bw})=0. \tag{19}$$

The source term of the energy equation (15) is given by

$$S_h=-4\pi K_a[I_b(T)-I_0]. \tag{20}$$

THE FINITE ELEMENT FORMULATION AND THE SOLUTION PROCEDURE

The finite element discretization equations are obtained by the Galerkin method.[17] Since the flows under consideration are highly convective, the transport equations containing convective terms are upwinded by a Petrov–Galerkin method,[18] which uses non-symmetric, continuous weighting functions. The finite elements used in this work are composite elements consisting of four quadrilaterals with bilinear interpolation for velocities and all other dependent variables (including the turbulent viscosity and density) except pressure (Figure 1). The pressure is linearly interpolated over the composite quadrilateral.

The segregated formulation of the Navier–Stokes equations

A segregated formulation is adopted for the solution of the momentum (1), (2) and continuity (4) equations. This approach is analogous to a well known finite difference procedure called SIMPLE.[19] Details of the finite element formulation and its applications in laminar incompressible flow problems can be found in Benim and Zinser.[20] The method is based on the

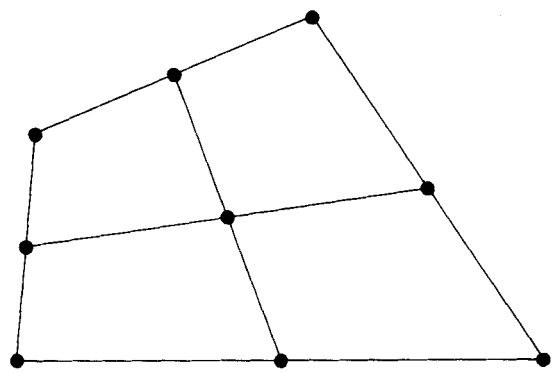

Figure 1. The finite element used

derivation of a discretization equation for pressure corrections p' directly from the discretized continuity equation, considering the relationships established between velocities and pressure in the discretized momentum equations. This equation in the present case takes the form

$$\int_\Omega H_i\left\{\left[\frac{1}{a_u}\left(\rho\frac{\partial N}{\partial x}+\frac{\partial \rho}{\partial x}N\right)\right]_j(b_u)_{jk}+\left[\frac{1}{a_v}\left(\rho\frac{\partial N}{\partial r}+\rho\frac{N}{r}+\frac{\partial \rho}{\partial r}N\right)\right]_j(b_v)_{jk}\right\}\mathrm{d}\Omega\, p'_k=g_i, \tag{21}$$

where

$$g_i=-\int_\Omega H_i\left[\rho\left(\frac{\partial u^*}{\partial x}+\frac{v^*}{r}+\frac{\partial v^*}{\partial r}\right)+u^*\frac{\partial \rho}{\partial x}+v^*\frac{\partial \rho}{\partial r}\right]\mathrm{d}\Omega. \tag{22}$$

N_i and H_i in (21) and (22) represent the shape functions for the velocity and pressure. The coefficients $(a_u)_i$ and $(a_v)_i$ denote the ith diagonal elements of the system matrices for u and v respectively. The terms $(b_u)_{ij}$ and $(b_v)_{ij}$ are the influence coefficients of the jth pressure node to u_i and v_i.[20] u^* and v^* denote the velocities based on the incorrect pressure field p^*. The corrections to the pressure field, which lead to a better satisfaction of the continuity equation, are obtained from equation (21). The velocities and pressures are subsequently corrected according to

$$u_i=u_i^*+\frac{1}{(a_u)_i}\sum_j(b_u)_{ij}p'_j, \tag{23}$$

$$v_i=v_i^*+\frac{1}{(a_v)_i}\sum_j(b_v)_{ij}p'_j, \tag{24}$$

$$p_i=p_i^*+\Omega_p p'_i. \tag{25}$$

An under-relaxation of the pressure is often necessary. Ω_p in (25) denotes the under-relaxation factor for the pressure. In this formulation, in contrast to the integrated formulation,[17] an absolutely continuity-satisfying velocity field at each iteration (solving a large system of equations) is not required. Rather, an asymptotic satisfaction of the continuity equation within the whole iterative procedure is sought. For highly non-linear problems and large meshes the present segregated formulation offers, we find, a more economical alternative than the integrated formulation.

The near-wall treatment

Turbulence dies out close to solid boundaries. The standard turbulence models based on high-Reynolds-number assumptions lose their validity in these regions. Here, the method of wall functions[7] provides a convenient alternative to model near-wall flows. In this approach it is assumed that the following equations hold within the wall layer:

$$\begin{aligned} u^+&=y^+ && \text{for } y^+<11{\cdot}6,\\ u^+&=(1/\kappa)\ln(Ey^+) && \text{for } y^+\geqslant 11{\cdot}6, \end{aligned} \tag{26}$$

$$k=u_\tau^2/C_\mathrm{D}^{1/2}, \tag{27}$$

$$\varepsilon=C_\mathrm{D}^{3/4}k^{3/2}/\kappa y, \tag{28}$$

which are derived under the main simplifying assumption that the shear stress is independent of the distance to the wall within the wall layer. Thus the boundary nodes can be placed not at the wall, but at a distance from the wall, the boundary conditions being derived from (26)–(28). To evaluate (26)–(28), the wall shear stress must be known. The present approach for the estimation of

the wall shear stress was discussed in Benim and Zinser.[8] A possible extension of the recursive shear stress formulae[8] for a wall element with irregular shape (Figure 2) is given below:

$$\tau_w = \begin{cases} \dfrac{\mu w_{p2}}{y_2} & \text{for } y_2^+ < 11{\cdot}6, \\ \dfrac{\kappa C_D^{1/4} \rho w_{p2} k_1^{1/2}}{\ln(E C_D^{1/4} \rho y_2 k_1^{1/2}/\mu)} & \text{for } y_2^+ \geqslant 11{\cdot}6 \end{cases} \tag{29}$$

In (29) w_p denotes the wall-parallel component of the velocity vector. For an inclined wall w_p must also replace u in (20). The velocity component normal to the wall can be obtained from continuity considerations.[8]

For the energy equation it is assumed that the heat transfer coefficients are known by experiments. The convective heat flux to the wall can then be prescribed as

$$q_w = \alpha_w (T - T_w), \tag{30}$$

where the wall temperatures are also assumed to be known as boundary conditions.

The solution algorithm

The important steps of the solution procedure can be summarized as follows:

Step 1. Guess initial fields for u, v, p, k, ε, μ_t, T, ρ, S_F.
Step 2. Solve (1) for u.
Step 3. Solve (2) for v.
Step 4. Solve (21) for p' and compute the new pressure field from (25).
Step 5. Correct velocity fields according to (23), (24).
Step 6. Solve (6) for k.
Step 7. Solve (7) for ε.
Step 8. Update μ_t and wall boundary conditions according to (5) and (26)–(28).
Step 9. Solve (9) for the concentration of fuel.
Step 10. Solve (10) for f.
Step 11. Calculate remaining concentration fields from (11), (12) and update S_F according to (14).

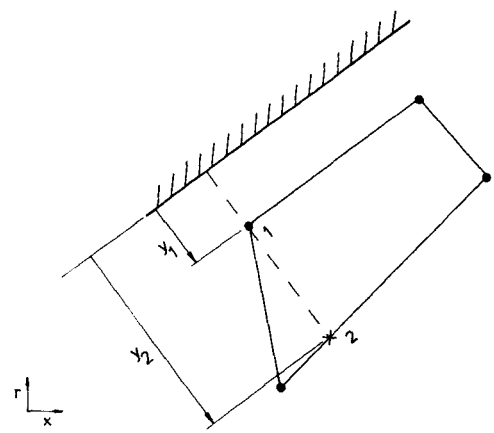

Figure 2. An element near the wall

Step 12. Solve (18) for I_0.
Step 13. Solve (15) for h.
Step 14. Compute the temperature and density fields from (16) and (17).
Step 15. Go to step 2 if convergence is not achieved.

The solution of the finite element discretization equations for each field variable is obtained by a direct solver using a band matrix storage mode. Under-relaxation is employed for u, v, p, k and ε subsequent to the solution of their discretization equations at steps 2, 3, 4, 6 and 7 in the above procedure. The μ_t, T, ρ and S_F fields are also under-relaxed. No under-relaxation is employed for m_j, f, I_0 and h. An optimization of the relaxation factors is not attempted. However, a few trials have indicated that the pressure field usually requires a heavier under-relaxation than the other variables. Wall boundary conditions are not directly under-relaxed. At initial iterations, a slight under-relaxation is used for the wall shear stress. No instability due to the wall model is observed.

NUMERICAL EXAMPLE

The present finite element formulation is assessed by investigating flame 29 of the M-2 trials[21] performed in the International Flame Research Foundation (IFRF). This is a non-swirling natural gas flame with axial fuel and coaxial air injection, and with 3000 kW thermal load. The furnace and the burner are sketched in Figure 3.

The inlet mass flow rate of the natural gas through the primary nozzle is 280 kg h^{-1}. Dry air with mass flow rate 3126 kg h^{-1} and oxygen with mass flow rate 170 kg h^{-1} are injected through the secondary nozzle. Detailed information about the experimental set-up can be found in Michelfelder and Lowes[21] and Michelfelder.[22]

The furnace does not have a circular cross-section (Figure 3, upper right sketch). Since the present mathematical model is two-dimensional axisymmetrical, the furnace geometry in the computations is approximated by a cylinder having the same cross-sectional area. This approximation should not impair the results too much, especially in the central zones where the important

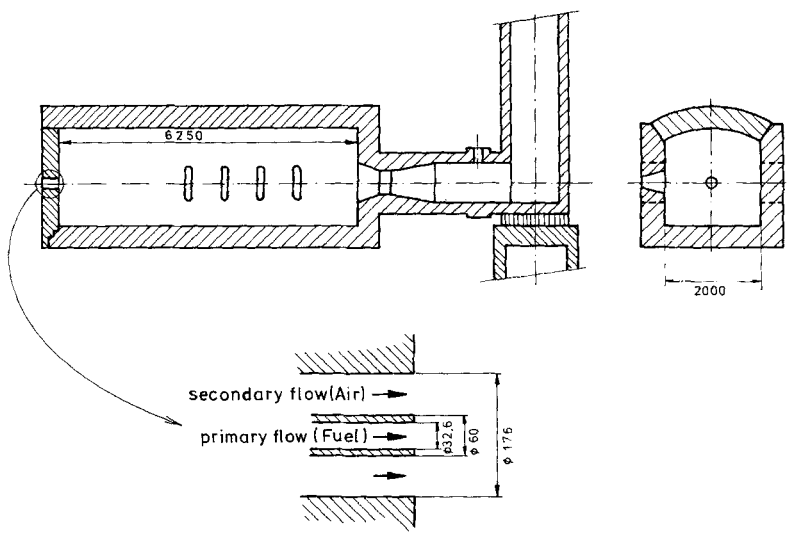

Figure 3. The furnace and the burner (dimensions in mm)

mixing procedures and chemical reactions take place, since the walls are quite far away from the burner. The finite element mesh consisting of the composite elements of Figure 2 is shown in Figure 4. Here the grid lines are squeezed near the inlet for a better resolution of the high gradients expected in this region. At the outlet boundary 'zero-traction' boundary conditions are applied for the Navier–Stokes equations. The following set of model constants is used in the present study:[7,16] $C_D = 0{\cdot}09$, $C_1 = 1{\cdot}43$, $C_2 = 1{\cdot}92$, $C_{1,EDC} = 4{\cdot}0$, $C_{2,EDC} = 2{\cdot}0$; $\sigma_{k,e} = 1{\cdot}0$, $\sigma_{\varepsilon,e} = 1{\cdot}3$, $\sigma_{m_i,e} = \sigma_{f,e} = \sigma_{h,e} = 0{\cdot}7$. It is known that the 'standard' constants do not perform very well for the round free jet.[7] In the present example, owing to the very large ratio of the furnace diameter to the jet diameter (Figure 3), the flow situation resembles, especially in the intial parts of the furnace, that of a free jet. Therefore the constants C_D and C_2 are modified for the first half of the furnace as; $C_D = 0{\cdot}075$, $C_2 = 1{\cdot}89$.

The finite difference results for comparisons are taken from Richter.[23] In this finite difference model a streamfunction–vorticity formulation with a k–W turbulence model was used. Different reaction models were employed.[23] For the present comparisons, the results[23] using a Pdf model are considered, since it is the most comparable one to the present reaction model (EDC). A 20×20 mesh[23] was used in the finite difference computations. This number is indeed small in comparison with the present finite element mesh (Figure 4); but the finite difference model has the advantage, due to the streamfunction–vorticity formulation, that the continuity equation is identically satisfied, in this variable density flow, whereas the finite element grid has only 16×16 pressure nodes within the furnace region due to the mixed interpolation (Figure 4).

The computed velocity field is plotted in Figure 5. As can be seen from the figure, the recirculation zone extends through the whole furnace.

Streamlines and the radial profiles of the streamfunction are presented in Figures 6 and 7 respectively. The finite element results show good agreement with experiment, whereas the finite difference curves predict too high values in the middle regions of the furnace. This superiority of the finite element results may partly be attributed to the better treatment of the momentum equations via the finer discretization.

The variation of the recirculating mass flow is shown in Figure 8. Again the finite element curve shows fair agreement with experiment, whereas the finite difference curve predicts too high values in the middle, as already implied by Figures 6 and 7.

Radial temperature profiles at four axial locations are presented in Figure 9. In most parts, the finite element results agree better with experiment.

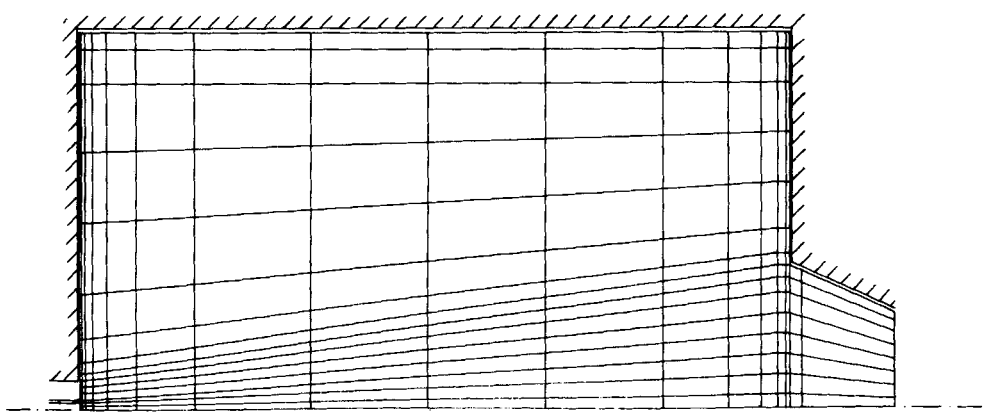

Figure 4. The finite element mesh

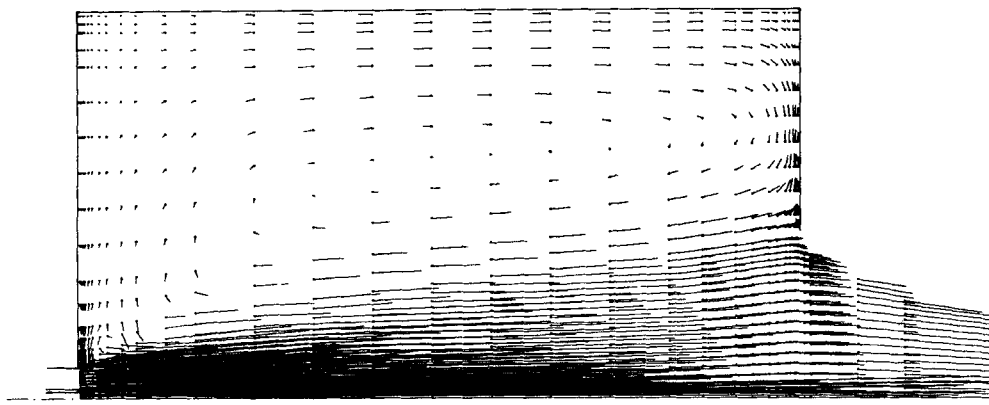

Figure 5. The velocity field

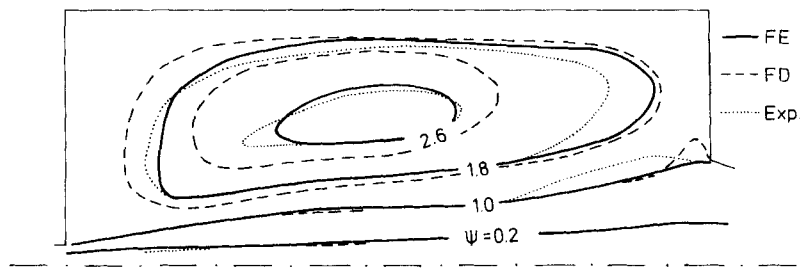

Figure 6. Streamlines

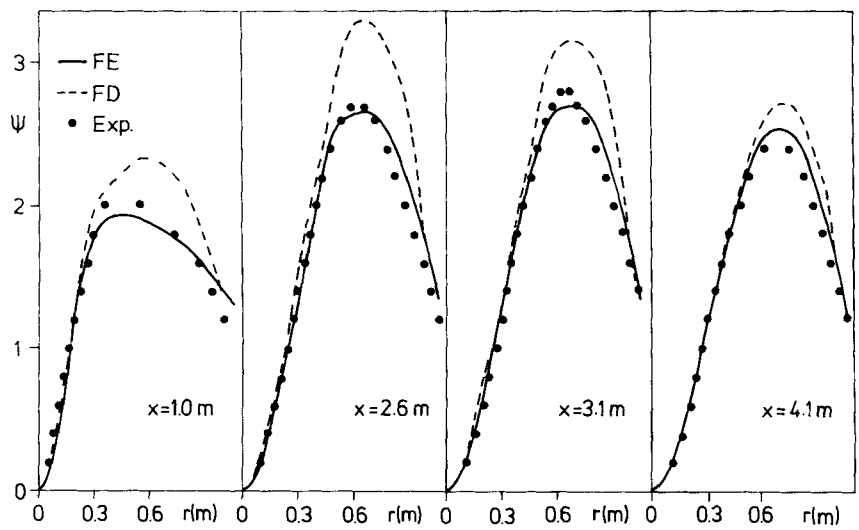

Figure 7. Radial profiles of the streamfunction

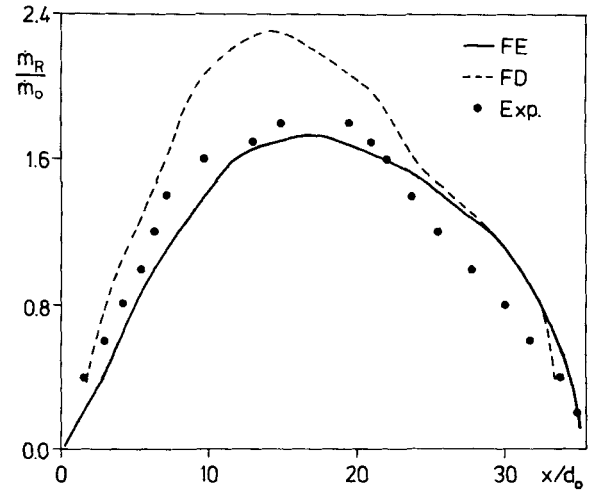

Figure 8. Variation of the recirculating mass flow with inlet distance

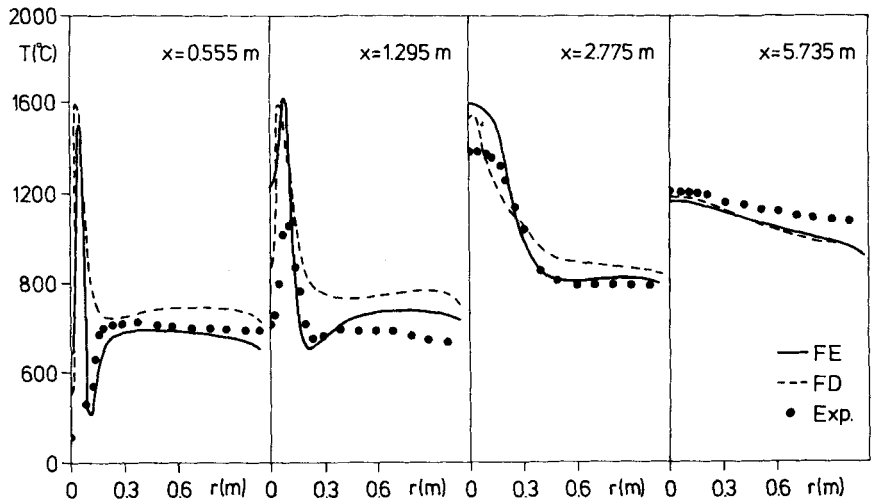

Figure 9. Radial temperature profiles

The variation of the incident radiative heat flux along the furnance wall is shown in Figure 10. In the present computations a constant absorption coefficient of 0·15 m^{-1} is assumed. The finite difference curve shown in Figure 10 is taken from Michelfelder[22] and was obtained by the zone method[9] using the measured gas temperatures and concentrations. The finite element curve is somewhat too 'smooth', but still gives a good estimation of the total heat flux.

Radial concentration profiles of CH_4 and O_2 near the reaction zone at two different axial locations are presented in Figure 11. A similar width of the reaction zone is predicted by the two methods, though the finite element curves generally show better agreement with experiment.

In Figure 12 the flow of the chemically bounded energy along the furnace length is presented. The finite element predictions again show quite good agreement with experiment.

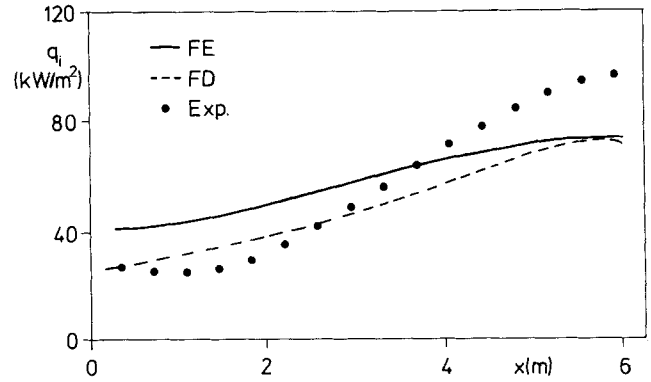

Figure 10. Variation of incident heat flux along the furnace wall

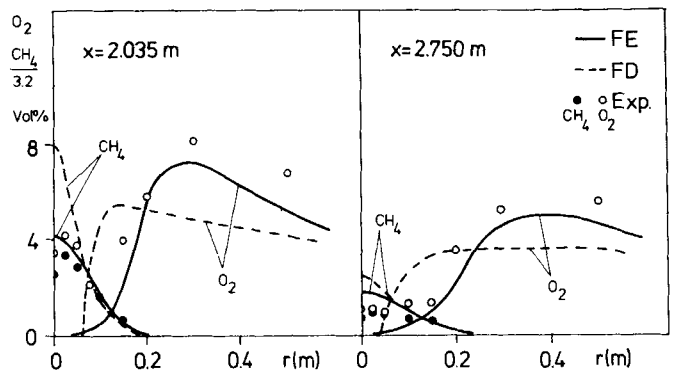

Figure 11. Radial concentration profiles

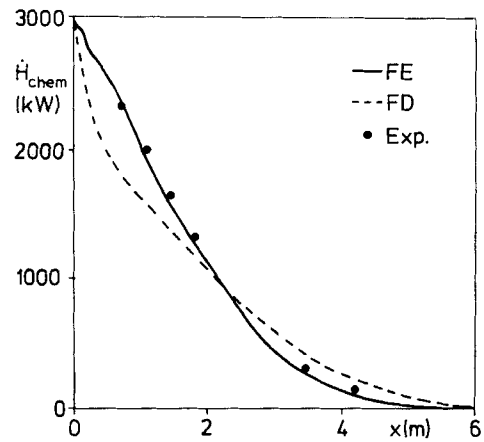

Figure 12. Variation of the integral burn-out along the furnace length

In the above computations a 2×2 Gaussian integration is employed to evaluate finite element integrals numerically. Owing the quadratic weighting functions, variable material properties (μ_t, ρ) and element distortions, the integrands in terms of the local co-ordinates are of quite high orders, for which a 2×2 integration is no longer exact. In order to see the influence of the numerical integration on accuracy, results were also obtained using a 3×3 Gaussian integration. No remarkable changes were observed in comparison with the 2×2 quadrature, showing that the 2×2 Gaussian integration is still accurate enough for the present case.

CONCLUSIONS

The present finite element model has been shown to predict succesfully the important features of enclosed turbulent diffusion flames. We expect that the incorporation of adaptive procedures will improve the prediction capability. The employment of different types of elements, and possible refinements in the radiation model or upwind procedures, will also be considered in future investigations.

ACKNOWLEDGEMENTS

This work was carried out within the TECFLAM Project on Mathematical Modelling and Laser Diagnostics of Technical Flames. Funding by the German Ministry of Research and Technology (BMFT) and the Federal Government of Baden-Württemberg is gratefully acknowledged.

NOMENCLATURE

$c_{p,j}$	integral specific heat of species j at constant pressure
C_1, C_2, C_D	constants in turbulence model
$C_{1,EDC}, C_{2,EDC}$	constants in reaction model
d_0	largest nozzle diameter
E	constant in near-wall velocity profile
F	fuel
h	specific enthalpy
$\dot{H}_{chem}$	integral flow of chemically bounded energy
I_0	direction-independent local mean radiation intensity
I_b	black body radiation intensity
k	turbulence kinetic energy
K_a	absorption coefficient
$\dot{m}$	mass rate of flow
m_j	mass concentration of species j
M_j	molecular weight of species j
n	normal direction
p	pressure
q	heat flux
r	radial co-ordinate
R	universal gas constant
T	temperature
u	axial velocity component
u_τ	shear velocity
v	radial velocity component

w_p	velocity component parallel to wall
x	axial co-ordinate
y	distance from wall

Greek Symbols

α	heat transfer coefficient
β	extinction coefficient
ε	dissipation rate of turbulence kinetic energy, emissivity
κ	von Karman's constant
μ	molecular viscosity
μ_t	turbulent viscosity
ν_j	stoichiometric coefficient of species j (mass basis)
ρ	density
σ	Prandtl–Schmidt number
τ	shear stress
Ψ	normalized streamfunction

Subscripts

e	effective
o	inlet
p	primary
R	recirculating
s	secondary
t	turbulent
w	wall

Superscripts

+	quantity non-dimensionalized by means of μ, τ_w and ρ

REFERENCES

1. D. B. Spalding, 'A general purpose computer program for multidimensional one- and two-phase flow', *J. Math. Comput. Simulation*, **XXIII**, 267–276 (1981).
2. N. S. Wilkes, 'Calculation of fluid flow using finite differences and the method of coordinate transformations', *HARWELL Report No. AERE-R11218*, 1984.
3. J. L. Sohn and T. J. Chung, 'Navier–Stokes mean flows interacting with vortex and acoustic oscillations', *Proc. 6th Int. Symp. on Finite Element Methods in Flow Problems*, 1986, pp. 145–170.
4. F. Benkhaldoun and B. Larrouturou, 'Adaptive calculations of wrinkled flames', *Proc. 6th Int. Symp. on Finite Element Methods in Flow Problems*, 1986, pp. 439–443.
5. P. Murray and G. F. Carey, 'Numerical computation of coupled viscous flow/transport problems: absorption of a gas by a moving fluid with reaction', *Proc. 6th Int. Symp. on Finite Element Methods in Flow Problems*, 1986, pp. 459–463.
6. A. Habbal, A. Deriveux, H. Guillard and B. Larrouturou, 'Explicit calculation of reactive flows with an upwind finite element hydrodynamical code', *INRIA Report No. 690*, 1987.
7. B. E. Launder and D. B. Spalding, 'The numerical computation of turbulent flows', *Comput. Methods Appl. Mech. Eng.*, **3**, 269–289 (1974).
8. A. C. Benim and W. Zinser, 'Investigation into the finite element analysis of confined turbulent flows using a k–ε model of turbulence', *Comput. Methods Appl. Mech. Eng.*, **51**, 507–523 (1985).
9. H. C. Hottel and A. F. Sarofim, *Radiative Transfer*, McGraw-Hill, New York, 1967.
10. W. Richter and G. Bauersfeld, 'Radiation models for use in complete mathematical furnace models', *Proc. IFRF 3rd Mem. Conf.*, 1974, Ch. II.
11. M. Krook, 'On the solution of equations of transfer', *Astrophys. J.*, **122**, 488–497 (1955).

12. A. C. Benim, 'A finite element solution of radiative heat transfer in participating media utilizing the moment method', *Comput. Methods Appl. Mech. Eng.*, **67**, 1–14 (1988).
13. J. O. Hinze, *Turbulence*, 2nd Edn, McGraw-Hill, New York, 1975.
14. R. W. Dibble and R. W. Schefer, 'Simultaneous measurements of velocity and scalars in a turbulent nonpremixed flame by combined laser Doppler Velocimetry and Laser Raman Scattering', *Proc. 4th Symp. on Turbulent Shear Flows*, 1983, Session 10.
15. A. D. Gosman, W. M. Pun, A. K. Runchal, D. B. Spalding and M. Wolfhstein, *Heat and Mass Transfer in Recirculating Flows*, Academic Press, London, 1969.
16. B. F. Magnussen and B. H. Hjertager, 'On mathematical modelling of turbulent combustion with special emphasis on soot formation and combustion', *Proc. 16th Symp. (Int.) Combustion*, Combustion Institute, 1976, pp. 719–729.
17. O. C. Zienkiewicz, *The Finite Element Method*, 3rd Edn, McGraw-Hill, London, 1977.
18. J. H. Heinrich, P. S. Huyakorn, O. C. Zienkiewicz and A. R. Mitchell, 'An 'upwind' finite element scheme for two-dimensional convective transport equation', *Int. j. numer. methods eng.*, **11**, 131–143 (1977).
19. S. V. Patankar, *Numerical Heat Transfer and Fluid Flow*, McGraw-Hill, New York, 1980.
20. A. C. Benim and W. Zinser, 'A segregated formulation of Navier–Stokes equations with finite elements', *Comput. Methods Appl. Mech. Eng.*, **57**, 233–237 (1986).
21. S. Michelfelder and T. M. Lowes, 'Report on the M-2 trials', *IFRF Report, Doc. No. F36/a/4*, 1974.
22. S. Michelfelder, 'Beitrag zur Berechnung des Abbrandes und der Wärmeübertragung von nichtleuchtenden Gasflammen', *Dissertation, University of Stuttgart*, 1976.
23. W. Richter, 'Mathematische Modelle Technischer Flammen', *Dissertation, University of Stuttgart*, 1978.